

CONTENTS

Introduction.

1. Beam shape aberration.
2. Long-wavelength de-focus.
 - 2.1 Effect at telescope focal surface.
 - 2.2 Detector focusing.
 - 2.3 Diffraction-limited fringe visibility at max OPD.
3. Long-wavelength coma.

Introduction.

It is taken as read that the SPIRE optical design is based on geometric optics (GO), valid because the beam size at the powered mirrors is many wavelengths across, e.g. at the shortest wavelength (0.25mm) the FTS pupil is $30\text{mm}/0.25 = 120$ wavelengths.

In this note we quantify the deviations from GO & their effect on performance in the worst case of $\lambda=0.5\text{mm}$ (centre of longest channel).

The starting or 'baseline' performance is that given by the GO aberrations e.g. ray-trace spot-sizes for image quality, and wave-front error. Since the ray-trace is purely geometric, and both systems are reflective, the GO effects apply similarly at all wavelengths. Here we list only the effects which occur in addition at long wavelength.

1. Beam shape aberration.

In the GO design the aberrations described are in wavefront of the far-field beam, leading to spot size in the focussed beam. The far-field beam shape is not considered, and each ray is effectively given equal flux (top-hat shape of far-field beam). If the system is used at long wavelength with gaussian beams, the beam shape ('apodisation' or 'slope-diffraction') affects the aberrations.

Furthermore, the use of off-axis ellipsoidal mirrors with diverging/converging beams means that the gaussian shape is distorted by reflection, giving both an asymmetry & an offset in the max. intensity, in the direction parallel to the plane of incidence. The effect increases with the beam divergence angles and the 'turning angle' of the mirror (ref.1).

This is a geometric effect and so is not wavelength-dependent at the mirror itself. However, the onward propagation is wavelength-dep't, since the reflected beam has its modal content changed (the asymmetry is equivalent to addition of modes of higher spatial order).

The effect of this in PHOT depends on the detector type used, and an asymmetry in the beam at the detector can lead to loss of detection efficiency. The asymmetry can be cancelled by arranging the fold angles of subsequent mirrors to be equal & opposite, i.e. a planar zig-zag train, and since PHOT has somewhat this form the asymmetry could be small.

In the FTS the additional worry would be if the interferometry used differing paths such that the final beams had differing shape. Thanks to the symmetry this is not the case. Also, the powered mirrors within the I/F arm (before & after the rooftop) have identical tilt and are in the asymmetry-cancelling orientation with respect to each other.

In the FTS fore-optics the beam asymmetry due to the train prior to the interferometer is more complicated, since the folding is in 3-d, and here cancellations are less likely. This means that the nominally collimated beam in the I/F path could have shape distortion. This shouldn't matter for the interferometry, as it occurs before the splitting, but it could have an effect on longer wavelength propagation & on FOV shape.

2. Long-wavelength de-focus.

We consider the beam imaging in terms of the transformation of wavefront radius of curvature (ROC) by each of the powered mirrors. In geometric optics the beam focus occurs at a distance from the mirror equal to the output ROC. For gaussian beams at longer wavelengths it occurs at a shorter distance z given by:

$$\text{ROC} = z(1+(z_0/z)^2) \quad (1)$$

Where $z_0 = \pi \cdot w_0^2 / \lambda$ is the confocal parameter.

2.1 Effect at telescope focal surface.

In the telescope, the defocus $\Delta z = z - \text{ROC}$, is small at the primary mirror because of its fast output beam (at $\lambda = 0.5\text{mm}$ $w_0 = 0.15\text{mm}$, giving $\Delta z \approx 0.01\text{mm}$).

At the secondary mirror, however we have $\text{ROC} = 2695\text{mm}$, $F = 8.6$, $\Delta z \approx -1.5\text{mm}$. Also, Δz increases with wavelength squared, and so reaches -6mm at $\lambda = 1\text{mm}$.

We have checked this effect in the model, and fig.1. shows the beam pattern at $\lambda = 0.5\text{mm}$, $\Delta z \approx -1.5\text{mm}$, for both gaussian & top-hat beams.

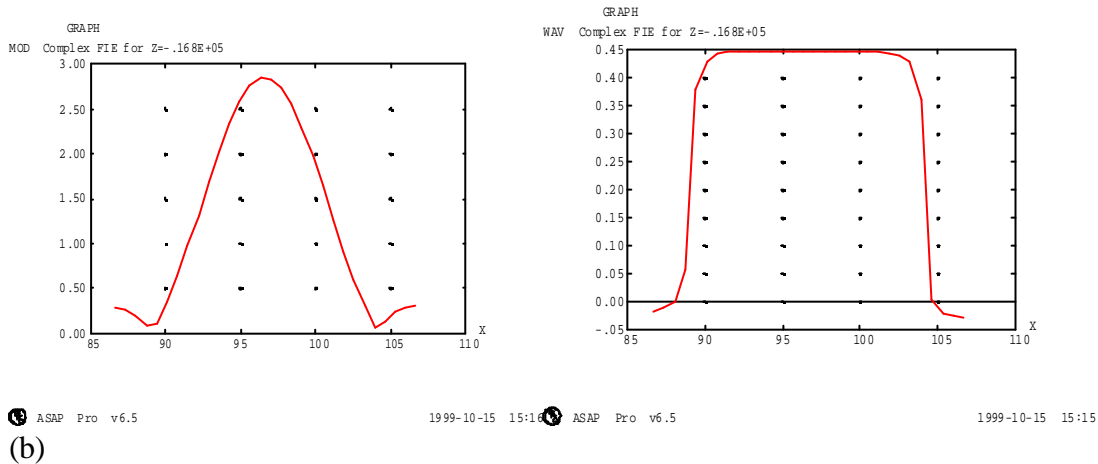
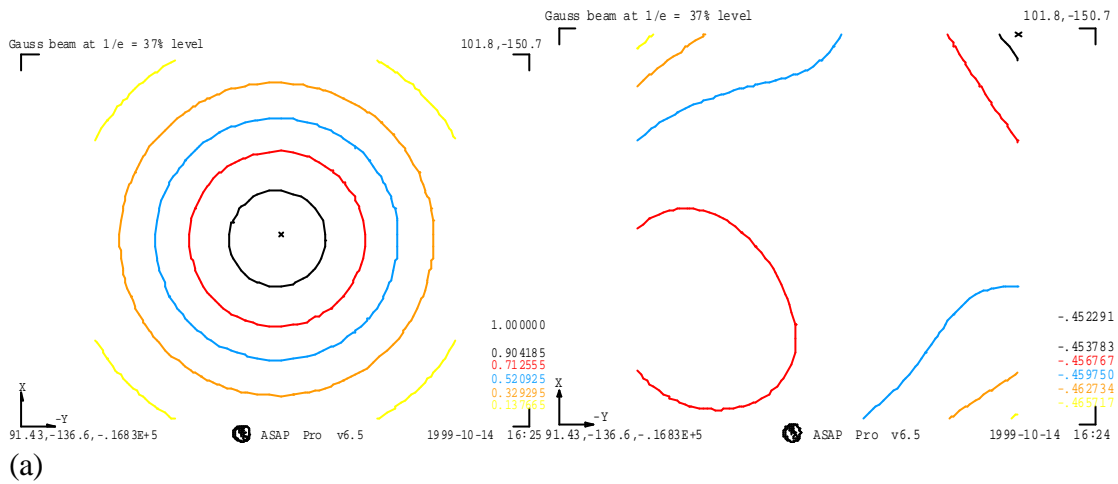


Fig.1. Beam patterns at telescope focus -1.5mm , for 21×21 rays. Modulus at left, wavefront at right. (a) clipped-gaussian case, shown in contour plots. (b) top-hat case, in cross-section, wavefront vertical scale is no. of waves.

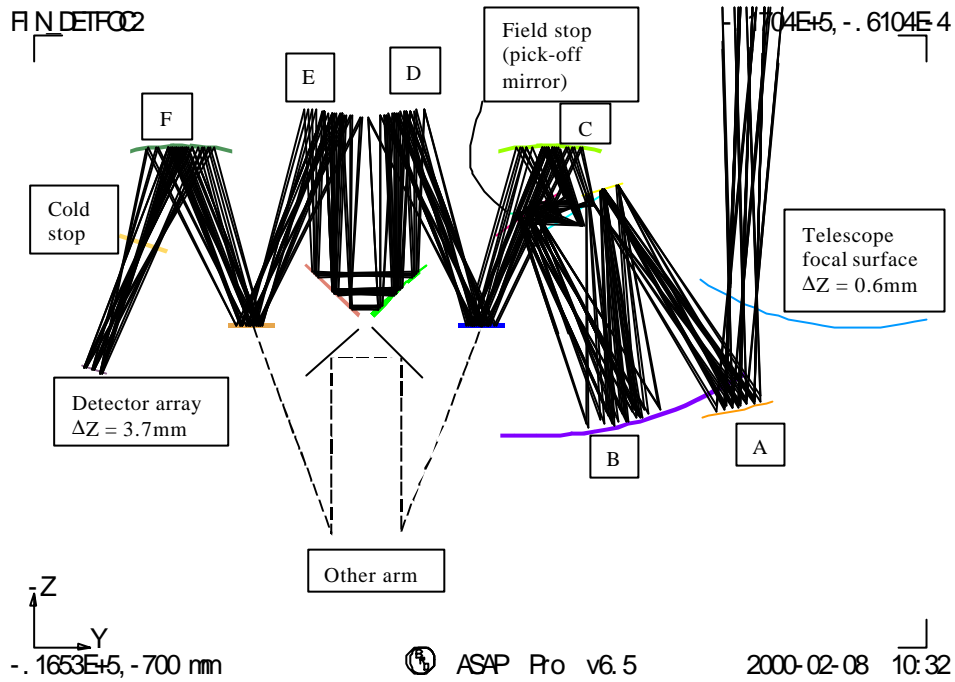
The main point to note is that the wavefront appears quite flat at this location (to within 0.003 waves over the $1/e$ waist aperture), in agreement with the above equation. The strong deviation, by 0.5 wavelengths at the edge of the beam in the top-hat case is associated with the first dark airy ring.

We have also tested the model at $\lambda=1\text{mm}$, and used the on-axis beam in the telescope, in order to exclude aberration effects. Comparisons of the top-hat & gaussian cases also show the same $\Delta z \approx -6$ mm effect in each, in agreement with (1). This implies that difference in beam shape from the gaussian case doesn't greatly affect the result.

2.2. FTS detector focus.

The deviation in long-wave focus (waist position) from GO focus continues through the system. In order to check the ASAP model, an independent first-order imaging model has been made. This takes the FTS design & 'unfolds' it, calculating the effective focal length of each powered mirror, and its position along the optical path, from its GO properties (object & image distances). The gaussian

beam imaging through the system is then calculated for comparison with the GO imaging (ref.2). The output from this model is shown in fig.2.



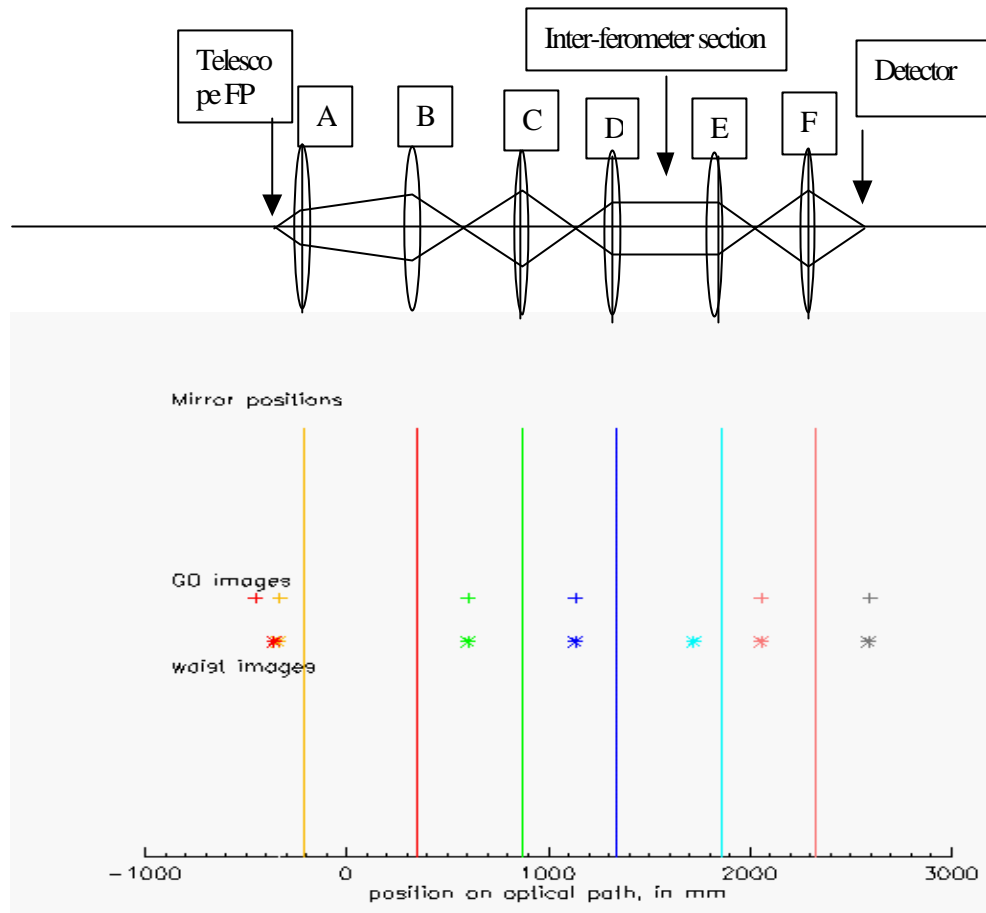
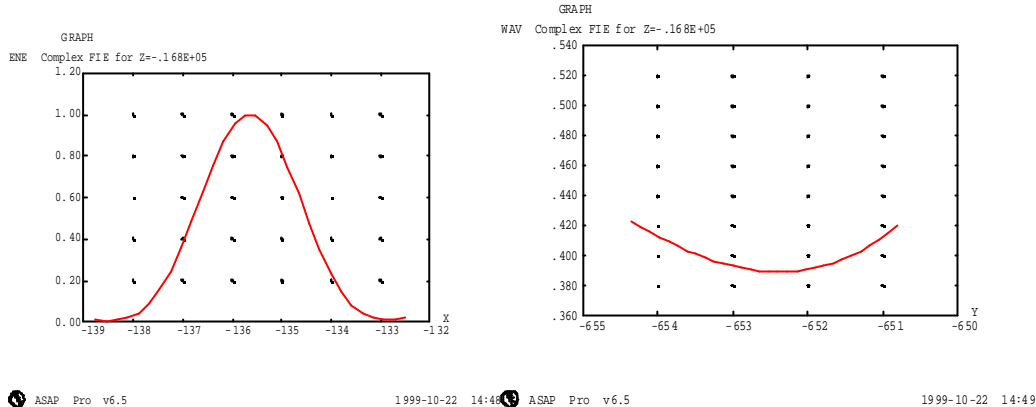


Fig.2. Image positions through the FTS optics train (shown in same colour as the corresponding mirror), for $\lambda=0.5\text{mm}$. The GO object position is at 0mm, the equivalent input waist position is at -1.5mm.

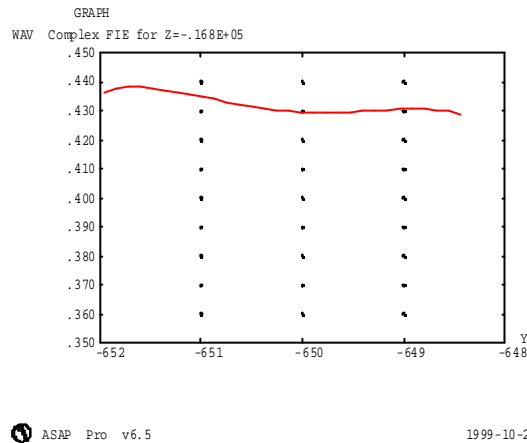
It can be seen that at this wavelength the waist position remains close to the GO focus. The exceptions are at the first mirror, where the imaged waist is close to the input waist, and in the collimated section, where there is no GO image (it is at minus infinity), but there is a waist image.

In the final output (FTS detector) the deviation of the waist from the GO image is $\Delta z=(196.25-200) = -3.75\text{mm}$.

The ASAP model output beam was investigated in this location, and results are shown in fig.3.



(a) beam at detector plane, i.e. GO focus (energy at left, wavefront at right)



(b) At detector plane-7mm.

Fig.3. Beam patterns at detector plane.

It is found that at the nominal detector plane the wavefront has significant curvature, and that this is largely corrected when we look at the beam at $\Delta z = -7\text{mm}$. The reason why this result is different from that of fig.2. may be because of the presence of aberrations in the wavefront, and unfortunately it is not possible to make this analysis without these aberrations being present.

The reverse propagation model through the whole system (inc. telescope) is shown in fig.4 for $\lambda = 0.5\text{mm}$.

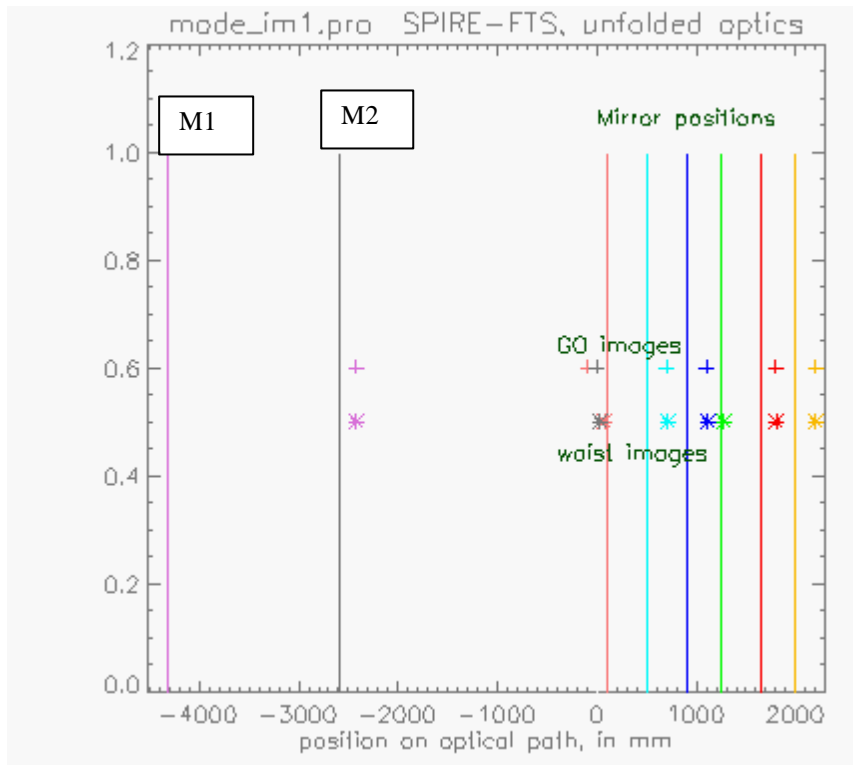


Fig.4. Reverse propagation model of FTS, with telescope included.

In this plot the GO and waist images appear within the instrument in similar locations as before. In object space (i.e. sky) the images do not appear in the plot because they are both at large distances. The GO image is at minus infinity, while the waist image would ideally lie at $-(M1 \text{ focal length})$ from M1 (ref.2), i.e. within the telescope. With the detector at the ideal long wavelength waist position, our model puts the output waist at -290km , and with a size of $w_0=1586.6\text{mm}$. With the detector set instead to the GO position, the long wavelength waist is shifted to $\Delta z=+8\text{mm}$ at telescope focus, and to -2850 km in object space with size $w_0=1623.7\text{mm}$. The corresponding beam confocal parameter is $z_0=16570\text{ km}$, and since this is much larger than the waist distance, the w_0 value is representative of the $1/e$ beam width at the telescope aperture.

Since the defocus effect gives an output waist size larger than the nominal, (rather than smaller), the effect of positioning the detector at GO will at long wavelength be to increase the level of clipping in the telescope (rather than decrease the spatial resolution).

2.3 Diffraction-limited fringe visibility at max OPD.

As well as the spatial resolution issue, there is the effect of interference mixing efficiency when the finite diffraction-limited divergence of the collimated beam (as indicated by its waist size & position) is combined with a non-zero OPD. In the above $\lambda=0.5\text{mm}$ model the beam waist in this region is $w_0=14\text{mm}$. This gives a confocal distance $z_0=1232\text{mm}$. At a distance z from the waist equal to the maximum OPD= 125mm , the wavefront ROC is 12.25metres , corresponding to a WFE (from

collimated) of 0.016λ at the edge of the beam ($1/e$ point). Such a WFE is not problematic but needs to be included in the budget.

3. Long-wavelength coma.

The above de-focus effect means that the object/image waist positions (or equivalently the ROC) of the mirror imaging changes with wavelength. For ellipsoidal mirrors this means a drift away from the focal points, and this can produce coma aberration.

(The configuration in which this effect is removed is that used in Fourier Optics (FO) as in the so-called gaussian-beam telescope, where the separations of focussing elements are kept as equal to the sum of their focal lengths, and the beam waists remain at the focal planes at all wavelengths).

This aberration effect isn't included in the GO ray-trace, but it can be dealt with by using ASAP beam decomposition to sample the ellipsoid. Alternatively it size could be checked analytically for the fundamental mode at each mirror (ref.1)

This effect has been sized for SPIRE (Ref.3) and found to be negligible.

References.

1. J.A.Murphy. "Distortion of a simple gaussian beam on reflection from off-axis ellipsoidal mirrors" International journal of infrared & MM-waves, Vol.8, No.9, pp. 1165-1187 (1987).
2. S.A.Self "Focussing of spherical gaussian beams" Appl. Opt. p.658, Vol.22, No.5 (1983).
3. "Beam pattern diffraction effects in design of SPIRE" SPIE Vol.4013. [SPIRE-RAL-PUB-000372](#).